Physical Modeling of Slag Penetration on the Refractories in a Static Magnetic Field

W. Zhang, A. Huang, Y. Zou, P. Lian, Y. Chen, H. Gu

Dedicated to the 10th Anniversary of refractories WORLDFORUM

Alumina based refractory is the important lining material in the process of steelmaking, and slag corrosion is one of the main forms of refractory wear. Electromagnetic field will affect the interface behaviour between refractories and molten slag because the molten slag has certain conductivity, meanwhile the wettability between refractories and molten slag is an important factor affecting slag corrosion. Therefore, a method of simulation experiment at room temperature was adopted, in which the molten slag was simulated by saturated NaCl solution composite, and alumina and resin materials were selected to simulate refractories in the static magnetic field, the effect of magnetic flux density on the slag penetration was investigated. The results showed that the effective electromagnetic damping formed in the static magnetic field, which can prevent the penetration of the molten slag to refractory materials. The higher the magnetic flux density is, the shallower the penetration will be, and the weaker the electrophoretic effect is. Furthermore, the inhibitory effect of slag penetration to the smaller pores is more obvious in the static magnetic field with same magnetic flux density. It is indicated that a static magnetic field can effectively regular or control the interface behaviour between refractory and molten slag to prolong the service life of refractories.

1 Introduction

Refractory materials are directly applied in high-temperature industry, including metallurgy, building materials, electricity, petrochemical industries, aerospace industries, defense construction, etc. They are necessarily basic materials, which guarantee the operation and technology development of the industries mentioned above, and play an important role in the quality of production and the efficient safe producing of thermal equipment including steelmaking. At present, alumina based refractory is one of the wear lining refractory materials mainly applied to steel refining, and the major wear mechanism is slag corrosion. More attention was paid to the process of electromagnetic materials as a new frontier interdisciplinary and research direction, and more extended innovations are competitively made all over the world, which have covered multiple emerging research fields including steel and nonferrous smelting, the preparation of nonmetallic materials and new materials [1–2]. Electromagnetic field widely exists in high-temperature process including metallurgy, of which thermal and force effects are important means to smelt new variety of steel and improve the quality of the steel [2–4]. Slag is in molten state at high temperatures, where there are a large number of ions and ion clusters. The electromagnetic field will significantly affect the trajectory and speed of the charged particles, which may lead to change in the interfacial behaviours between slag and refractories, and change the slag corrosion mechanism of refractories, etc.

Aneziris et al. [5] showed that electromagnetic could change the wettability of slag and magnesium oxide and promote electron transition and exchange, and the accompanying interfacial reaction. It influenced the formation and distribution of the high-temperature phases or phases with low-melting point and accelerated the dissolution of magnesium oxide in the molten slag. Khoroshavin et al. [6] theoretically discussed the influences of electronic technology on the performance of refractory materials and predicted what electromagnetic would af-

Wenxuan Zhang, Ao Huang, Yongshun Zou, Pengfei Lian, Yunke Chen, Huangzhi Gu
The State Key Laboratory of Refractories and Metallurgy
Wuhan University of Science and Technology
Wuhan, Hubei 430081
China

Corresponding author: *Ao Huang*
E-mail: huangao@wust.edu.cn

Keywords: static magnetic field, slag penetration resistance, physical modeling, electromagnetic damping

Received: 29.06.2018
Accepted: 30.07.2018

Tab. 1 Compositions of simulated molten slag [mass-%]

NaCl	Distilled Water	Ethanol	Osmotic Imaging Agent
18,17	73,82	7,62	0,39

fect the electron motion in redox reaction. Pötschke [7] proposed that electromagnetic field could influence penetration behaviour of the molten slag, and the double electronic shell between refractory and slag at high temperature should be considered, which could change wettability of the slag and refractory. Aneziris et al. [8] have studied the interfacial behaviour between MgO refractory and slag in an electric field. It was confirmed that electric field affected the interfacial reaction between refractories and slag, and found that the wetting angle between slag and refractory increased with the increasing of the electric field at high temperature, and the permeability decreased. Also, the phase composition of the interface was changed in electric field.

Li et al. [9–10] carried out the experiment on slag resistance of MgO–C refractory in an alternating electromagnetic field, and found that electromagnetic field promoted high-iron slag penetration and wear of the MgO–C refractory due to carbonaceous material's conductivity and Fe^{2+} influenced greatly. Simultaneously, electromagnetic filed could accelerate the dissolution of MgO into the slag and reduce the emission drag of $Mg_{(g)}$, which inhibited the formation of MgO's dense layer at the interface.

Li et al. [11] investigated the effect of electromagnetic field on the corrosion of magnesia-calcia refractories by using induction furnace, the results showed that the iron ion of Fe_2O_3 in magnesia-calcia refractories could diffuse in the field of electromagnetic, and the corrosion and penetration of slag to magnesia-calcia refractories was more serious than those without electromagnetic fields.

Huang et al. [12–13] showed that static magnetic field could inhibit corrosion and penetration of slag to porous alumina materials, then they explored the change of slag properties and its corrosion behaviours to refractories in a static magnetic field using numerical simulation combined with experimental verification, and they found that, static magnetic field could contribute to improving refractory slag resistance.

Therefore, the paper is based on the characteristics and range of slag wettability on refractories, alumina and resin materials were selected as simulated refractories, and physical modeling experiment was applied to investigate the conductive slag penetrability on refractories in a static magnetic field, which has great theoretical value and practical significance for analysing the service behaviour of refractory in the static magnetic field, reducing resources consumption and improving the quality of steel.

2 Experimental

2.1 Raw materials

Two types of fused alumina powders ($Al_2O_3 \geq 99,5$ mass-%, $d_{50} = 74$ µm and 45 µm, Jiangsu Jinxing New Material Co., Ltd./CN), and reactive alumina power ($Al_2O_3 \geq 99,5$ mass-%, $d_{50} = 2,5$ µm, Zhejiang Zili Co., Ltd./CN) were used as the alumina source materials; polyvinyl alcohol (PVA, Changchun Chemical Co., Ltd./CN), and glycerin (Tianjin Zhiyuan Chemical Reagent Co., Ltd./CN) were used as the binder and additive for fabricating alumina ceramic disc; Epoxy Resin (EP, Shandong De Yuan Epoxy Technology Co., Ltd./CN) and triethanolamine (TEOA, Shanghai Sino Principle International Trading Co., Ltd./CN) were used as the raw material and curing agent for fabricating resin disc.

Sodium chloride (AR, Tianjin Bodi Co, Ltd./CN), distilled water, ethanol (AR, Sinopharm Chemical Reagent Co., Ltd./CN), and osmotic imaging agent (DPT-5, Shanghai Xinmeida Co., Ltd./CN) were used as the solute-solvent solution composite to simulate molten slag with a certain conductivity.

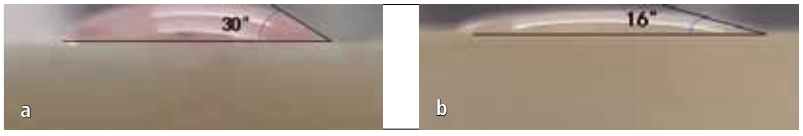

Fig. 1 a–b Wetting angles of simulated molten slag and (a) alumina disc, (b) resin disc

2.2 Preparation of simulated molten slag

Electromagnetic field is an important means of regulating and controlling conductive fluid, of which the key parameter is the fluid conductivity. While slag is of melting state at high temperature, it has certain conductivity. Considering that conductivity may be changed in the static magnetic field, a simulated slag solution with similar conductivity range to molten slag needs to be configured in the following experiments.

The conductivity of a solution is proportional to its concentration, which presents a certain linear relationship and is shown as below [14]:

$$K = 0,9861 \times 10^5 C + 18,464 \qquad \text{(eq. 1)}$$

where, K is the solution conductivity ($\mu S \cdot cm^{-1}$), C is the solution concentration ($mol \cdot l^{-1}$).

At room temperature of 10 °C, the concentration of saturated NaCl solution is 3,376 $mol \cdot l^{-1}$. Based on the equation 1, its conductivity is $33,3 \times 10^4$ $\mu S \cdot cm^{-1}$, which is within the range of molten slag conductivity from $23,5 \times 10^4$–$102,6 \times 10^4$ $\mu S \cdot cm^{-1}$ in 1400–1600 °C [15].

So, a saturated NaCl solution was chosen as conductive liquid and ethanol was introduced to ensure homogeneous dispersion of osmotic imaging agent. The mixed solution composite was stirred uniformly and prepared before each experiment. The compositions of the simulated molten slag are shown in the Tab. 1.

2.3 Sample preparation

According to the conventional permeability formulas, it can be seen that the wettability between refractories and molten slag is an important factor affecting slag corrosion. The key parameter is the wetting angle θ of molten slag and refractories at the corrosion interface. Refractories are usually composed of oxides, and slag is also basically made of oxides, which has a strong wettability with refractory materials.

Considering the effect of wetting angle on slag penetration to refractories, the experiment needs samples whose range of wetting angles of simulated molten slag is similar with that between molten slag and refractories, of which the wetting angle may vary from 10–30° [16]. Therefore, the wet-

ting angle of the solid-liquid interface was measured by dropping simulated solution on the surface of alumina ceramic and resin discs. The results are shown in Fig. 1.

As can be seen from Fig. 1, the wetting angle of the simulated molten slag and the resin disc was 16°, the wetting angle of the simulated molten slag and the alumina disc was 30°. In view of refractory matrix being the weak link to its slag penetration and corrosion, it is indicated that both alumina and resin discs can be used to simulate refractory matrix in the experiments.

2.3.1 Alumina disc preparation

The two types of fused alumina powders and reactive alumina powers were weighted and premixed with mass proportion 2 : 2 : 1, then PVA was added with 5 mass-%, plane-type mill was applied to mix for 10 min. Then it was axial pressed to form green body under the pressure of 200 MPa, which size was Φ 40 mm × 60 mm. Next it was dried to constant weight at 110 °C and fired at 1650 °C for 3 h.

2.3.2 Resin disc preparation

Epoxy resin and triethanolamine were mixed in a volume ratio of 4 : 1 until it was pellucid and casted into a Φ 40 × 6 mm disc sample. Then it was vacuum dried at 110 °C for 12 and cured at 80 °C for 6 h. After cooling to room temperature, the surface of the resin disc was polished, and holes with uniform distribution and the same depth were drilled with a pointed cone to simulate defects or large pores on the surface of refractory materials. The pore diameter was 1 ± 0,2 mm.

2.4 Experimental procedure

As shown in Fig. 2, a Direct Current (DC) power supply with steady adjustable voltage 0,0–64,4 V and 1500 magnetic coils with diameter of 0,2 mm were applied to produce a static magnetic field. Teslameter (TD-8620, Tianheng Measurement and Control Co,. Ltd./CN) was applied to measure magnetic flux density.

Firstly the sample disc was put into the simulated molten slag in a beaker, and teslameter should be made zero adjustment. Then, a static magnetic field was produced, which was perpendicular to the surface of the disc and kept a constant magnetic flux density for 10 min. After that, the disc was taken out to clean its redundant agent on the surface, developed for 7 min, and recorded by a camera. After each test, disc sample was washed under clear water firstly, and then put in a supersonic cleaner for next test. In order to explore the influence of magnetic flux density on the simulated slag penetration, an electron microscope (Nova 400 NanoSEM, FEI Company/US) was applied to observe and analyse the microstructure of the sample for unobserved results by naked eyes.

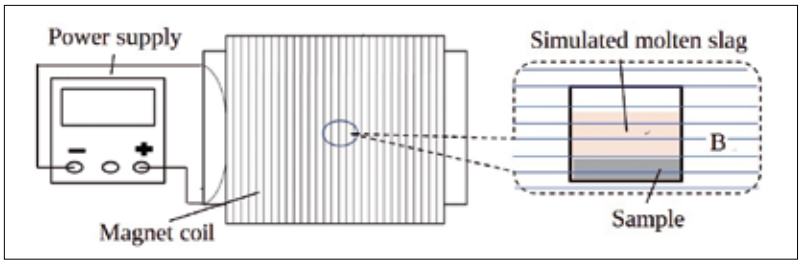

Fig. 2 Schematic diagram of the experimental devices

3 Results and discussion

3.1 The effect of magnetic flux density

It can be clearly observed at the macro level, the average size of pores on the surface of alumina disc was smaller than that of resin disc. Therefore, in the penetration test, a slightly larger magnetic flux density was selected to 0,2 mT for the resin disc. Fig. 3 shows the change of simulated slag penetration on the alumina disc followed magnetic flux density increasing at the range of 0~0,16 mT. Fig. 4 shows the change of simulated slag penetration on the resin disc followed magnetic flux density increasing at the range of 0~0,20 mT.

It can be seen in Fig. 3–4, due to the uneven size and distribution of the pores on the alumina disc and the tolerance of self-made pores on the resin disc, there were some differences in the coloration on the both alumina and resin discs and it indicated that pore size has an important effect on the slag penetration resistance in a static magnetic field.

In the static magnetic field with smaller magnetic flux density, the coloration showed a general trend of reducing as the magnetic flux density increased for the same pores. In particular, when magnetic flux density increased from 0,07 mT to 0,16 mT, the colour gradually became lighter as the magnetic flux density increased. It suggested that the smaller magnetic flux density could inhibit the slag penetration. However, the colour was abnormally darker when the magnetic flux density was 0,12 mT for resin disc and 0,07 mT for alumina disc, which showed that the increase of magnetic flux density from 0,02 mT to 0,07 mT failed to enhance the inhibition of the simulated slag penetration. The magnetic field caused the central ions to collide with the water molecules when they moved, which leaded energy reducing and a sudden drop in the conductivity of the NaCl solution. It reduced the ability of the static magnetic field to inhibit the simulated slag penetration by electrophoretic effect [17].

Fig. 5 shows the change of simulated slag penetration on the alumina disc followed magnetic flux density increasing at the range of 0~1,75 mT. In view of the test results that when the magnetic flux density was bigger than or equal 0,75 mT, the penetration resistance of the resin disc has no significant change. Therefore, the following discussion on the effect of the range of magnetic flux density was limited to 0,75 mT for the resin sample. Fig. 6 shows the change of simulated slag penetration on the resin disc followed magnetic flux density increasing at the range of 0~0,75 mT.

As shown in Fig. 5–6, in the condition of relatively stronger magnetic field, the coloration of the discs showed an obvious trend of lighting generally as the magnetic flux density increased with ignoring its weak electrophoretic effect. The colour change was much larger than that in the condition of smaller magnetic flux density described above. When the magnetic flux density was bigger than or equal 1,25 mT for the alumina disc, the colour had turned significantly lighter, and while the magnetic flux density increased to 1,75 mT, the coloration

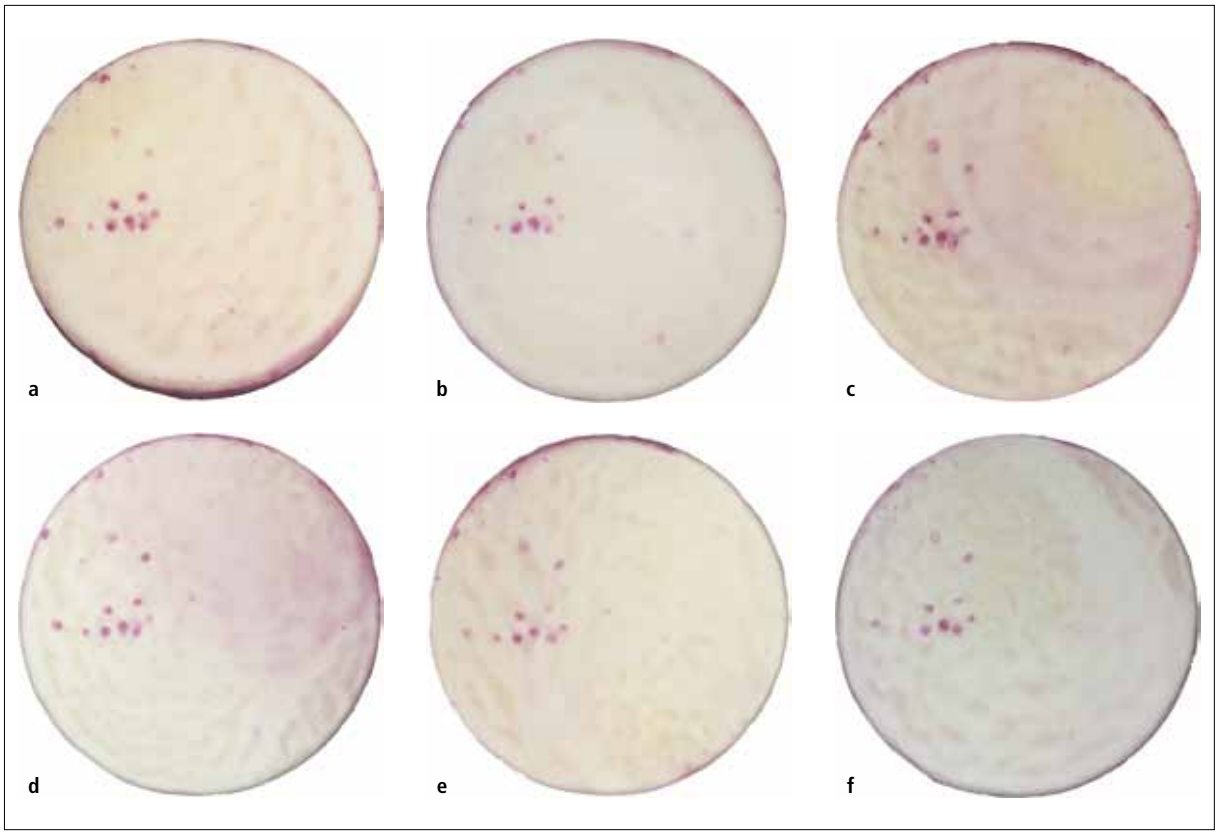

Fig. 3 a–f Coloration change on the penetrated alumina disc with increasing of the magnetic flux density (~0,16 mT)

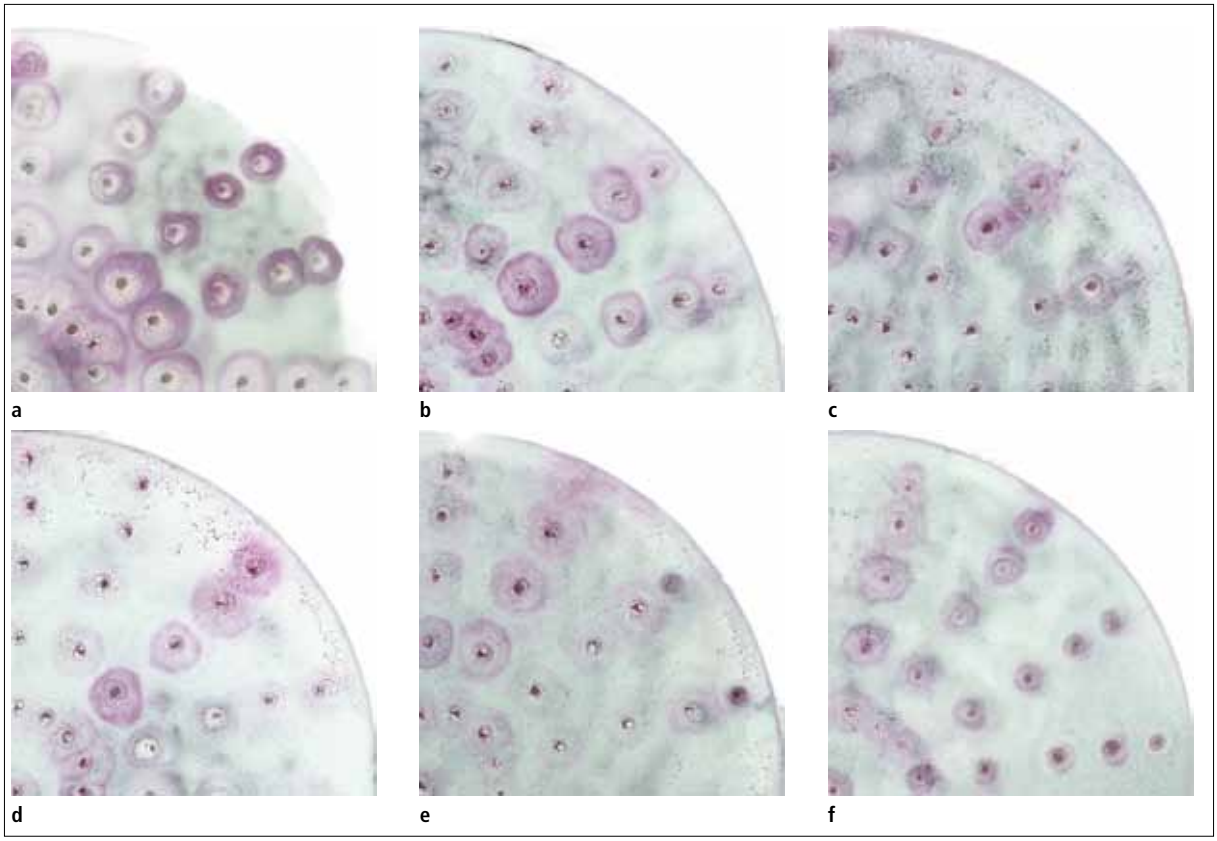

Fig. 4 a–f Coloration change on the penetrated resin disc with increasing of the magnetic flux density (~0,20 mT)

Fig. 5 a–e Coloration change on the penetrated alumina disc with increasing of the magnetic flux density (~1,75 mT)

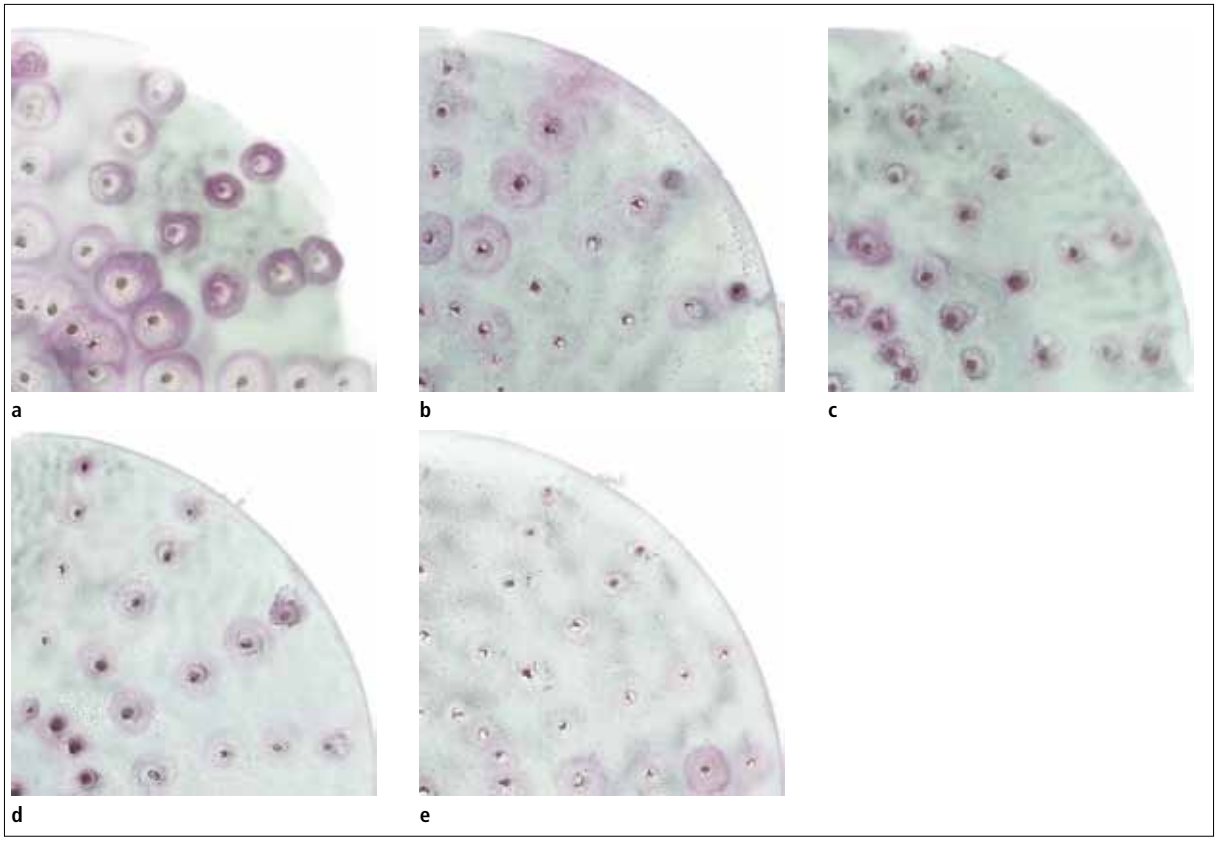

Fig. 6 a–e Coloration change on the penetrated resin disc with increasing of the magnetic flux density (~0,75 mT)

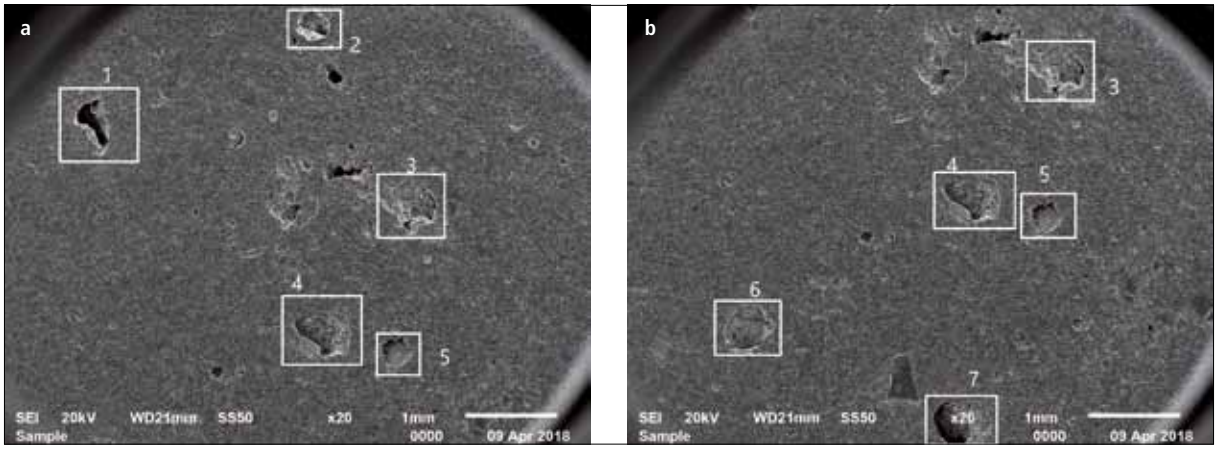

Fig. 7 a–b Surface microstructures of the alumina disc

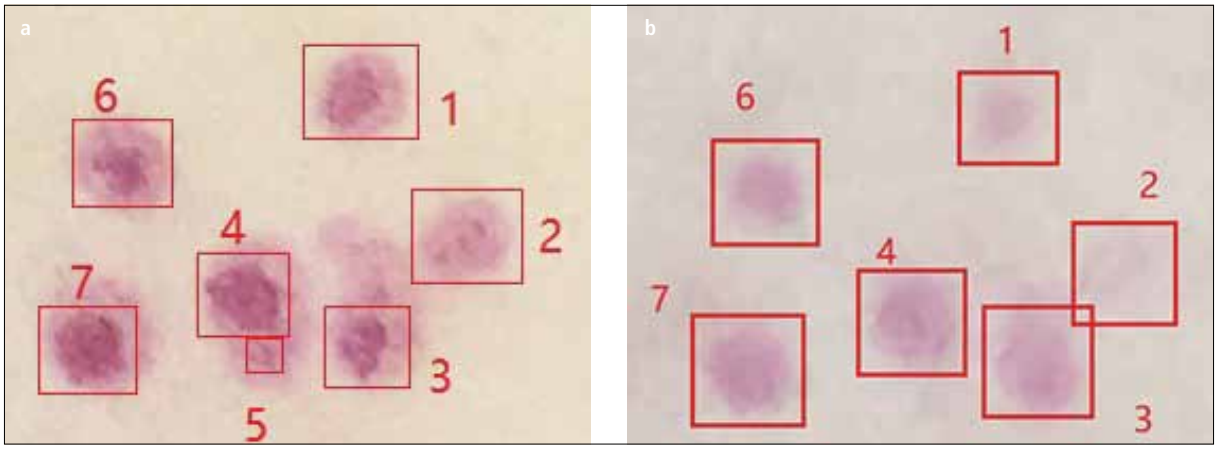

Fig. 8 a–b Surface macroscopic photos of the penetrated alumina disc with magnetic flux density of (a) 0,00 mT, and (b) 1,75 mT

was basically faded. When the magnetic flux density was bigger than or equal to 0,45 mT for resin disc, the colour had also turned significantly lighter, and while the magnetic flux density increased to 0,75 mT, the simulated slag penetration into the resin disc was inhibited greatly. It indicated that applying the static magnetic field with a relatively larger magnetic flux density can inhibit the slag penetration more effectively.

The charged ions in the simulated molten slag were affected by the Lorentz force F in the magnetic field, which is represented as:

$$F = Q \times V \times B \qquad \text{(eq. 2)}$$

where, F is the Lorentz force [N]; Q is the electric charge of charged ions [C]; V is the velocity of charged ions [m/s]; B is the magnetic flux density [T]. When B became bigger, the larger the Lorentz force F was, so the resistance to ions was greater in this case.

Furthermore, when the magnetic flux density increased, the conductivity of the NaCl solution also increased, and the resistance to charge flow f_r (N) was smaller. According to Newton's second law:

$$\sum F_1 = \mathrm{F} + f_r = m \times a \qquad \text{(eq. 3)}$$

Where, $\sum F_1$ is total external force on the charged ions which acts as resistance (N); m is weight [kg]; a is acceleration velocity [m/s^2]. In summary, when the magnetic flux density is increased, the inhibition of the slag penetration is greatly enhanced.

3.2 Microstructure analysis

Since the pores on the surface of the alumina disc cannot be identified and quantified by naked eye, the microstructure of the alumina disc was observed by SEM. Fig. 7 shows the microscopic view on the surface of the alumina disc, and Fig. 8 shows the macroscopic appearance corresponding with microscopic view of the alumina disc. The equivalent radius of pores from no. 1 to no. 7 were calculated using the graphic method according to Fig. 7, there were as $R_1 = 0{,}1875$ mm, $R_2 = 0{,}1719$ mm, $R_3 = 0{,}2656$ mm, $R_4 = 0{,}2813$mm, $R_5 = 0{,}1563$ mm, $R_6 = 0{,}2578$ mm, $R_7 = 0{,}2619$ mm.

For the resin disc, the average pore size R_r is 0,5 mm. The pores are sorted based on their radius, and the resulting order is $R_5 < R_2 < R_1 < R_6 < R_7 < R_3 < R_6 < R_r$. It can be clearly observed from Fig. 8 that the smaller pore size on the surface of the alumina disc is, the lighter the colour becomes, and the smaller colour distribution shows; for the larger aperture, the darker and larger distribution the colour is.

It indicated that coloration or penetration depth and pore size had a certain relationship, according to capillary theory:

$$h = 2\,\gamma\cos\theta/(\rho g R) \qquad \text{(eq. 4)}$$

where, h is the penetration depth due to the capillary phenomenon [m]; γ is the surface

tension [N/m]; θ is contact angle [°]; ρ is liquid density [kg/m^3]; g is acceleration of gravity [m/s^2]; R is capillary radius [m].
Because the colour represents the volume of simulated molten slag with coloration agent contained in the pores,

$$v = S \times h \quad \text{(eq. 5)}$$

where, v is the volume of simulated molten slag with coloration agent contained in the pore (m^3); S is the area of the pore (m^2);

$$S = \pi R^2 \quad \text{(eq. 6)}$$

It can be obtained from equations (4)~(6):

$$v = 2\ \gamma\pi R\cos\theta/(\rho g) \quad \text{(eq. 7)}$$

From the equation 7, it can be concluded that when the pore size is smaller, the coloration agent absorbed in the pores was less, the lighter the colour was, and the smaller the scope of the coloration points was.
As shown in Fig. 5, when magnetic flux density increased to 1,75 mT, the colour on the local surface of the sample was basically faded and the inhibition effect was obvious. It also revealed that the electromagnetic damping had a better effect on the inhibition of the simulated slag penetration in the pores with a smaller pore size.

3.3 Penetration analysis

It can be analysed from the Fig. 1 that wetting angle (16°) of the simulated molten slag with resin disc was smaller than that (30°) with alumina disc.
When the two kinds of samples were in the magnetic field with the same magnetic flux density which had the same inhibitory effect on the slag penetration, it is found that the simulated slag penetration to the samples in the static magnetic field was affected by wetting angle at the solid-liquid interface, the pore size of the sample surface, and the magnetic flux density of the applied magnetic field.
When the magnetic field is applied, the actual penetration depth will be shallower than the theoretical depth,

$$h` = 2\gamma\cos\theta/(\rho gR) - (Q \times V \times B + f_r) \times t^2/2m \quad \text{(eq. 8)}$$

where, $h`$ is the modified penetration depth due to the capillary phenomenon [m]; t is the penetration time [s]. The modified volume of simulated molten slag with coloration agent contained in the actual infiltrated pore,

$$v` = S \times h` \quad \text{(eq. 9)}$$

In conjunction with equations (6), (8) and (9),

$$v` = 2\gamma\pi R\cos\theta/(\rho g) - 50\pi R^2(QVB + f_r)/m \quad \text{(eq. 10)}$$

For different discs in the static magnetic field with the same magnetic flux density, both the pore size and wetting angle affected the slag penetration. According to the equation 7, as the wetting angle θ increases in the range of 0–90°, the wettability gets worse, the depth of simulated slag penetration reduced within a same time.
Penetration has a reverse relationship with wetting angle (0°~90°) and a positive correlation with pore size. Therefore, for both samples, the pore size of resin disc $R_r = 0{,}5$ mm, the maximum pore size of alumina disc $R_{max} = 0{,}2578$ mm, surface tension of the simulated molten slag $\gamma = 0{,}1107$ N/m, density of the simulated molten slag $\rho = 3{,}296$ kg/m^3 [18], $g = 9{,}8$ m/s^2, it can be obtained $v_{resin} = 2{,}0699 \times 10^{-5}$ m^3, $v_{alumina} = 1{,}5285 \times 10^{-6}$ m^3. Therefore, according to the forementioned analysis results, most resin pores have a greater degree of penetration than that of alumina's smallest pores.

4 Industrial test

According to the above modeling and analysis, a preliminary industrial test was applied on the purging plug for gas blowing in a refining ladle for special steel. A plug was equipped with a static magnetic field with gas cooling, of which the magnetic flux density was more than 20 mT tested in the room temperature. The service life of the plug was increased more than 20 % from 19–23 heats. It indicated that the static magnetic field with a certain magnetic flux density was promising for improving the service efficiency of refractories especially functional materials.

5 Conclusions

(1) In the condition of static magnetic field, when the magnetic flux density was smaller, with the increasing of the magnetic flux density, the penetration depth of the simulated molten slag was generally reduced. However, due to the electrophoretic effect, the inhibition ability of static magnetic field to slag infiltration was slightly weaker.
(2) When the magnetic flux density increases, the electrophoretic effect gradually turns weaker. With the increasing of the magnetic flux density, the penetration of the simulated molten slag to the discs can be more effectively suppressed.
(3) When the magnetic flux density increased to a certain value, the colour on the local surface of the discs was basically faded. When the pores have a certain distribution, the discoloration of the pores becomes more obvious. It can be concluded that the static magnetic field has better inhibition effect on the simulated slag penetration and is promising for improving the service efficiency of refractories especially functional materials.

References

[1] Li, G.; Wang, H.: Electromagnetic process of materials. Jiangsu University Press, 2014
[2] Wang, Q.; et al.: New electromagnetic technology. Science Press, 2015
[3] Mapelli, C.; Baragiola, S.: Development of solidification microstructures in continuously cast billets of boron and resulphurised steel grades. Ironmaking & Steelmaking **35** (2008) 441–451
[4] Tsukaguchi, Y.; et al.: Development of swirling flow submerged entry nozzles for slab casting. ISIJ Int. **50** (2010) 721–729
[5] Aneziris, C.G.; Hampel, M.: Microstructured and electro-assisted high-temperature wettability of MgO in contact with a silicate slag-based on fayalite. Int. J. of Appl. Ceram. Technol. **5** (2008) 469–479
[6] Khoroshavin, B.; Shcherbatskii. B.: An electronic technology for refractories based on the periodic law. Refractories and Industrial Ceramics **46** (2005) 344–351
[7] Pötschke, J.: Does electrowetting influence slag infiltration? 51st Int. Coll. on Refractories for Metallurgy, Eurogress Aachen, 2008, 144–146
[8] Aneziris, G.; Hampel, M.: Microstructured and electro-assisted high-temperature wettability of MgO in contact with a silicate slag-based on fayalite. Int. J. of Applied Ceram. Technol. **5** (2008) 469–479

[9] Li, X.; Zhu, B.; Wang, T.: Effect of electromagnetic field on slag corrosion resistance of low carbon MgO-C refractories. Ceramics Int. **38** (2012) 2105–2109

[10] Li, X.; Zhu, B.; Wang, T.: Electromagnetic field effects on the formation of MgO dense layer in low carbon MgO-C refractories. Ceramics Int. **38** (2012) 2883–2887

[11] Li, S.; Ma, B., Li, H.: Corrosion and penetration behaviors of molten slag on the magnesia calcia refractories under electromagnetic field. Proc. of the 11th China Iron and Steel Conference, Beijing, 2017, 1127

[12] Lian, P.; et al.: Characteristics and corrosion behavior on refractories of molten slag under electromagnetic field. Proc. 15th Unified Int. Technical Conf. on Refractories, Santiago, Chile, 2017, 641–644

[13] Huang, A.; et al.: Modeling and experiment of slag corrosion on the lightweight alumina refractory with static magnetic field facing green metallurgy. J. of Mining and Metallurgy, Section B: Metallurgy **54** (2018) [2]

[14] Yao, J.; et al.: Research on the empirical formula of the line between conductivity and solution concentration function. China Sci. and Technol. Expo **20** (2008) [5–6]

[15] Liang, L.; et al.: Electrical conductivity measurement of electroslag using four-probe electrode with AC conductometer. J. of Northeastern Institute of Technology, Natural Sci. Ed. (1985) [3] 74–80

[16] Shen, P.: Study on interfacial phenomenon among steel-slag-lining refractory system. University of Science and Technology Beijing, 2017

[17] Cheng, S.; et al.: Experimental research on effects of magnetic fields on the conductivity of NaCI solutions. High Technol. Letters **20** (2010) 1091–1095

[18] Xi, H.: Physical properties of sodium chloride solution. J. of Tianjin Institute of Light Industry (1997) [2] 72–74